




# Intracortical synchronization pattern on the preclinical and clinical stages of absence epilepsy (analysis of wavelet bicoherence in WAG/Rij rats)

Evgenia Sitnikova<sup>1,a</sup>, Elizaveta Rutskova<sup>1,b</sup>, Kirill Smirnov<sup>1,c</sup>, Anastasiya Runnova<sup>2,3,4,d</sup>, and Maksim Zhuravlev<sup>2,3,4,e</sup> 

<sup>1</sup> Laboratory of Neuroontogenesis, Institute of Higher Nervous Activity and Neurophysiology of Russian Academy of Sciences, Moscow 117485, Russia

<sup>2</sup> Center for Coordination of Fundamental Scientific Activities, National Medical Research Center for Therapy and Preventive Medicine, Moscow 101990, Russia

<sup>3</sup> Institute of Cardiological Research, Saratov State Medical University, Saratov 410005, Russia

<sup>4</sup> Institute of Physics, Saratov State University, Saratov 410012, Russia

Received 20 August 2022 / Accepted 26 October 2022 / Published online 9 November 2022

© The Author(s), under exclusive licence to EDP Sciences, Springer-Verlag GmbH Germany, part of Springer Nature 2022

**Abstract** Here we examine the intracortical synchronization pattern in freely moving WAG/Rij rats (valid animal model of absence epilepsy). In all rats, electrocorticograms were recorded at the age 5 and 9 months (i.e., preclinical and clinical stages of absence epilepsy in epileptic subjects). To assess intracortical synchronization pattern, we measured wavelet bicoherence in unilateral (fronto-frontal) and bilateral (fronto-occipital) electrode pairs in five non-overlapping frequency bands (“1–4 Hz”; “5–9 Hz”; “9–12 Hz”; “12–14 Hz”; “14–20 Hz”) and two additional bands “0.5–1.5 Hz”; “10–14 Hz” bands. Bilateral fronto-frontal synchronization in epileptic subjects was lower than in non-epileptic ones only on the clinical stage of absence epilepsy. Unilateral fronto-occipital synchronization in epileptic rats was lower (“5–9 Hz” and “10–14 Hz”) than in non-epileptic ones only on preclinical stage. This finding may be interpreted as a marker of thalamo-cortical impairment associated with epileptogenic processes underlying long-term progression of absence epilepsy. We construct plots of synchronization patterns or diagnostic maps, which can be used for early diagnosis of absence epilepsy in predisposed subjects.

## 1 Introduction

Absence epilepsy is a genetic (idiopathic) generalized epilepsy [1]. Absence seizures are non-convulsive, and they are accompanied by bilaterally synchronous spike-wave discharges (SWDs) in electroencephalogram (EEG) [2–5]. It is well accepted that SWDs are originated from thalamo-cortical neuronal network [6–14]. Some reports proved the intuitively clear notion: hypersynchronous SWDs are linked to a high synchronization within the thalamo-cortical circuitry [15, 16]. Low attention was paid to periods between seizures (interictal periods), as long as in accordance to the

classical point of view SWDs occurred “on a normal background activity” (Commission on Classification and Terminology of the International League Against Epilepsy, 1989), suggesting that the baseline EEG in absence epilepsy was almost healthy. More recently, several types of advanced brain networks analysis have been performed in patients with absence epilepsy demonstrating altered functional brain connectivity during resting state [8, 17, 18]. Analysis of brain connectivity may help to extract valuable information about hidden processes during “healthy” periods intricately linked to absence epilepsy. Advanced techniques of EEG-fMRI studies led to controversial conclusions about functional connectivity, likely because of inconsistent epileptic sub-syndromes, influences of age and medications, and physiological changes and technical errors [17]. The abovementioned reasons seem to impede further analysis of functional brain connectivity in patients with absence epilepsy. Here we examined

<sup>a</sup> e-mail: eu.sitnikova@ihna.ru

<sup>b</sup> e-mail: erutskova@gmail.com

<sup>c</sup> e-mail: kirillsmirnov@ihna.ru

<sup>d</sup> e-mail: a.e.runnova@gmail.com

<sup>e</sup> e-mail: zhuravlevmo@gmail.com (corresponding author)

electrocorticograms (ECoG) in genetically prone drug-naive WAG/Rij rats with the same genetic background, but different epileptic phenotypes (see below).

Here we study functional associations between brain regions using a nonlinear analysis of intracortical synchronization, which was based on a multiscale calculation of wavelet bicoherence. Nonlinear estimates of oscillatory processes are in high demand for biological and medical research, because these are appropriate methods for analyzing complex and non-stationary signals. On the contrary, the classical Fourier transform method that is often used for frequency and phase analysis provides correct outcomes under condition that analyzed signal is stationary and lasts significantly longer [19–21]. In this sense, the nonlinear wavelet transform provides ample opportunities for studying non-stationary and noisy electroencephalographic signals, as demonstrated, for example, in [22–25].

WAG/Rij rats is a well-recognized valid model of absence epilepsy, in which SWDs spontaneously appear in the ECoG [26–29]. Our Institution has the own breeding colony of WAG/Rij rats derived from Nijmegen University (Netherlands) in the middle of 90th. The IHNA's colony of WAG/Rij rats showed a high variety of SWD number and duration; moreover, some rats do not develop spike-wave seizures throughout the entire life [30]. All WAG/Rij rats in IHNA's colony have a genetic predisposition to absence epilepsy, but only some of them develop seizures. In subjects with the typical epileptic phenotype, the first immature SWDs appear at the age of 5 months (i.e., later than in the original colony in Nijmegen University), and the fully blown SWDs appears at the age of 9 months [31–34]. Considering that the presence of SWDs in EEG/ECoG is the main diagnostic evidence of absence epilepsy, the age of 5 months 'epileptic' WAG/Rij rats is considered as a preclinical stage of absence epilepsy.

It is well known that sleep–wake states regulation mechanisms effectively control the incidence of SWDs, and SWDs readily appear during passive waking state (restless immobility), drowsiness and non-rapid eye movement sleep (NREM sleep) [10, 35–40]. In contrast, active waking and rapid eye movement sleep (REM sleep) are much less favorable for the occurrence of SWDs. Here we recorded ECoG in freely moving epileptic and non-epileptic rats and analysed "healthy" interictal periods in search of intracortical synchronization patterns features specific to absence epilepsy. We automatically recognized two states: NREM sleep and Wake/REM sleep, and examined intracortical synchronization for these states separately (due to methodological restrictions we were not able to distinguish between wakefulness and REM sleep).

By comparing brain activity in rats of epileptic and non-epileptic phenotypes at two ages using wavelet bicoherence analysis, we could (1) evaluate special features of brain activity that accompany mature absence epilepsy in rats; (2) check for hallmarks of forthcoming absence epilepsy development.

## 2 Methods

### 2.1 Animals

Rats were obtained from a breeding colony of the Institute of Higher Nervous Activity and Neurophysiology RAS (Moscow, Russia). Ten adult male WAG/Rij rats were used in this study. Experiments were performed in accordance with EU Directive 2010/63/EU and approved by our institution's animal ethics committee (Protocol 4 from 26 October 2021). Rats were kept in standard conditions with a 12:12 light/dark cycle with lights on at 8 a.m. and had free access to rat chow and tap water.

### 2.2 ECoG recording and analysis

All rats were implanted with epidural screw electrodes at the age of 4.5 months (body weight 250–300 g). Stereotactic surgery was performed under chloral hydrate anesthesia (i.p. injections 325 mg/kg, 4% solution in 0.9% NaCl). ECoG was recorded in freely moving WAG/Rij rats. Three active electrodes (stainless steel screws with shaft length = 2.0 mm, head diameter = 2.0 mm, shaft diameter = 0.8 mm) were implanted symmetrically over the left and right frontal cortex (AP 2; L +/- 2.5) and over the right occipital cortex (AP -6; L3). Coordinates are given in mm relative to the bregma. Reference screw electrode was implanted over right cerebellum. Multi-channel amplifier (PowerLab 4/35, LabChart 8.0 software, ADInstruments) was used, signals were digitized with 400 samples/second/per channel and stored in the hard disk.

ECoG analysis was performed in 3 h periods from 21:00 to 23:59 (beginning of dark period). Three states were detected: Spike-wave discharges (SWDs), NREM sleep and Wake/REM sleep. SWDs in ECoG represented a sequence of synchronous high-voltage spikes and waves with a frequency of 8–10 Hz and minimal duration of 1.5 s. Examples of SWDs as recorded in epileptic rat ID = A5K8 are shown in Fig. 1A, B, where immature SWDs was at the age of 5 months (Fig. 1A) lower intrinsic frequency and shorter duration than in fully blown SWDs recorded at age of 9 months (Fig. 1B). Next, the state of NREM sleep (Fig. 1C) and Wake/REM sleep (Fig. 1D) were detected automatically using wavelet-based algorithm described elsewhere [41, 42]. In brief, we used continuous wavelet transformation in a floating time window to assess the wavelet energy in three ECoG channels (FrL, FrR, OcR). Multichannel energy ratios were calculated and, using the quantitative estimate of amplitude we introduced detection criteria:

- For each animal, individual threshold coefficients for the beginning and completion of NREM sleep and SWDs were automatically estimated.
- Detection of periods of NREM sleep and Wake/REM sleep was based on calculation of the value of wavelet energy in band [5; 10] Hz integrating over a 1/2 s time

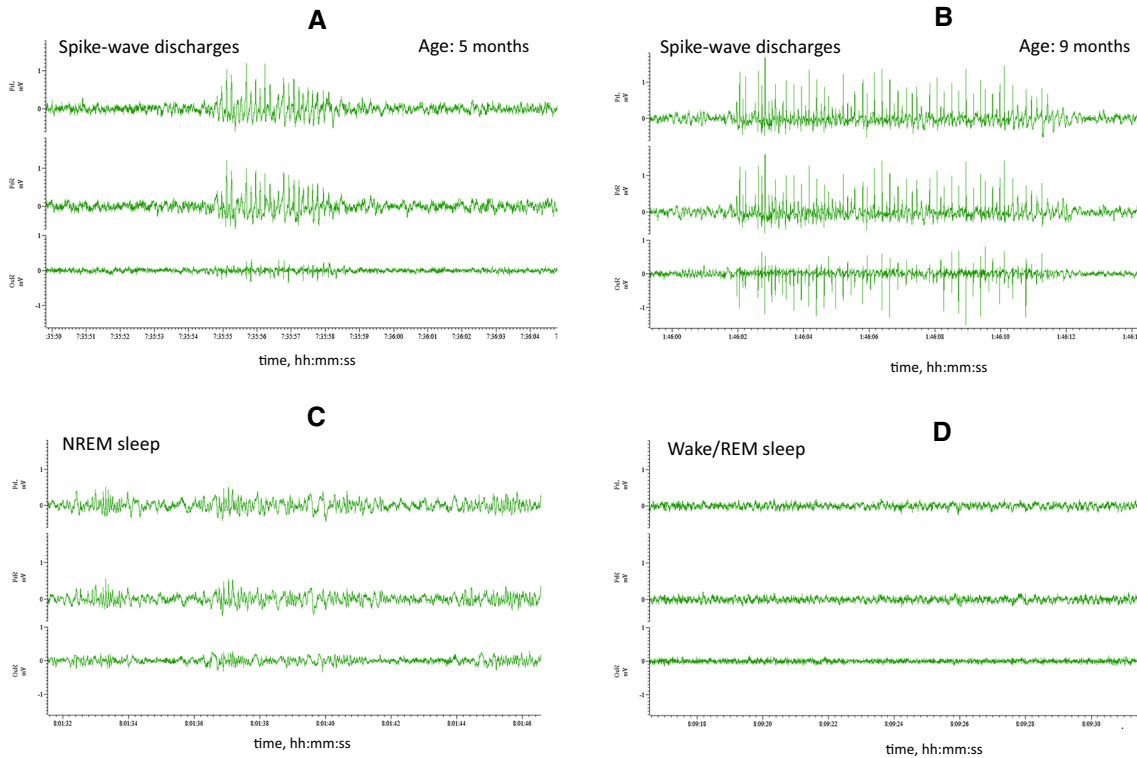


**Fig. 1** Examples of raw ECoG recorded in freely moving WAG/Rij rat (male, epileptic rat ID = A5K8). The signal was recorded with three active electrodes implanted epidurally to the following locations: *FrL* frontal left, *FrR* frontal right, *OcR* occipital right. **A** Immature SWDs at the age of 5 months; **B** immature SWDs at the age of 5 months; **C**, **D** ECoG recordings made during REM and Wake/REM at the age of 9 months

window. The time dependence of this integral wavelet energy was compared with threshold values to mark the sleep and wakefulness per ECoG recordings of animals.

- SWDs were detected when the ratio of integrated wavelet energy values, calculated in bands [2.5; 4.5], [10.5; 12.5] and [15; 18] Hz, exceeded individually estimated threshold values. To increase the sensitivity of the method and exclude false diagnosis of atypical sleep spindles, the amplitude pattern of extreme points in primary wavelet detected fragments of ECoG signals was additionally assessed.

### 2.3 Wavelet bicoherence analysis

Wavelet bicoherence analysis was used to assess intracortical synchronization between unilateral channels (symmetrical left and right frontal channels, FrL and FrR, Fig. 1) and between bilateral channels (right frontal and occipital cortical channels, FrR and OcR, Fig. 1).

Synchronization strength between ECoG signals was calculated with using of the wavelet bicoherence method [43–45]. This method is widely used to work with biomedical signals, including brain activity signals [46, 47]. We calculate the complex-valued wavelet coefficients  $W(f, t_0)$  for each ECoG channel as

$$W_{FrL}(f, t_0) = \sqrt{f} \cdot \int_{t_0-4/f}^{t_0+4/f} FrL(t) \cdot \psi^*(f \cdot (t - t_0)) \cdot dt, \tag{1}$$

$$W_{FrR}(f, t_0) = \sqrt{f} \cdot \int_{t_0-4/f}^{t_0+4/f} FrR(t) \cdot \psi^*(f \cdot (t - t_0)) \cdot dt, \tag{2}$$

$$W_{OcR}(f, t_0) = \sqrt{f} \cdot \int_{t_0-4/f}^{t_0+4/f} OcR(t) \cdot \psi^*(f \cdot (t - t_0)) \cdot dt, \tag{3}$$

where  $t_0$  specifies the wavelet location on the time axis and “\*” denotes the complex conjugation, and  $\psi(f, t)$  is the mother wavelet function. We use the standard Morlet wavelet, which is often utilized for processing of biological signals [48]:

$$\psi(f \cdot (t - t_0)) = \sqrt{f} \cdot e^{-1/4} \cdot \exp(i \cdot \omega_0 \cdot f \cdot (t - t_0)) \cdot \exp\left(-f^2 \cdot (t - t_0)^2 / 2\right), \tag{4}$$

where  $\omega_0$  is the wavelet scaling parameter and  $i$  is an imaginary unit. Well known that parameter  $\omega_0 = 2\pi$  in the continuous wavelet transformation (CWT) provides an optimal time-frequency resolution of EEG signal [49, 50].

Synchronization was evaluated for each pair of channels, i. e., three numerical characteristics were calculated for each pair of channels. The scheme of

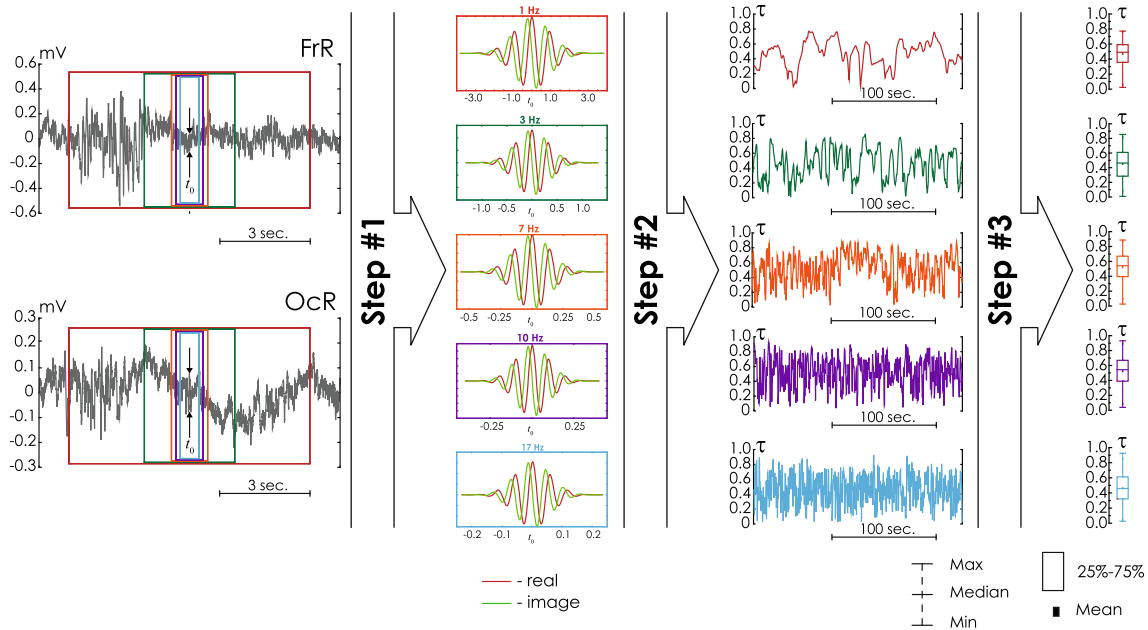


**Fig. 2** The scheme illustrating the method of wavelet bicoherence calculation. It includes three steps: (Step 1): decomposition of two ECoG signals in the predetermined frequency bands; (Step 2): the outcomes of decomposed signal; (Step 3): mean values of wavelet bicoherence

the synchronization estimation method is shown in Fig. 2. To measure the degree of coherence between ECoG signals we use the corresponding complex-valued wavelet coefficients as  $W_{FrL}(f, t_0) = \alpha_{FrL}(f, t_0) + i \cdot \beta_{FrL}(f, t_0)$ ,  $W_{FrR}(f, t_0) = \alpha_{FrR}(f, t_0) + i \cdot \beta_{FrR}(f, t_0)$  and  $W_{OcR}(f, t_0) = \alpha_{OcR}(f, t_0) + i \cdot \beta_{OcR}(f, t_0)$ .

The calculation of the synchronization characteristic is shown in detail for two channels, FrR and OcR. For other pairs of channels, the degree of coherence was calculated analogically. Similar to [47, 51] the coefficients  $Re[\tau_{FrR/OcR}(f, t)]$  and  $Im[\tau_{FrR/OcR}(f, t)]$  represented as real and imaginary parts of mutual wavelet spectrum can be calculated as

$$Re[\tau_{FrR/OcR}(f, t)] = \frac{\alpha_{FrR}(f, t) \cdot \alpha_{OcR}(f, t) + \beta_{FrR}(f, t) \cdot \beta_{OcR}(f, t)}{\sqrt{\alpha_{FrR}^2(f, t) + \beta_{FrR}^2(f, t)} \cdot \sqrt{\alpha_{OcR}^2(f, t) + \beta_{OcR}^2(f, t)}} \tag{5}$$

and

$$Im[\tau_{FrR/OcR}(f, t)] = \frac{\beta_{FrR}(f, t) \cdot \alpha_{OcR}(f, t) - \alpha_{FrR}(f, t) \cdot \beta_{OcR}(f, t)}{\sqrt{\alpha_{FrR}^2(f, t) + \beta_{FrR}^2(f, t)} \cdot \sqrt{\alpha_{OcR}^2(f, t) + \beta_{OcR}^2(f, t)}} \tag{6}$$

Further, the amount of synchronization between channels FrR and OcR was calculated for each frequency  $f$  as

$$\tau_{FrR/OcR}(f, t) = \sqrt{(\text{Re}[\tau_{FrR/OcR}(f, t)])^2 + (\text{Im}[\tau_{FrR/OcR}(f, t)])^2} \tag{7}$$

In the numerical calculation of the wavelet energy (1)–(3) for each estimated frequency  $f$ , the time window was chosen to  $8/f$ , as shown in Fig. 2. With single wavelet bicoherence,  $\tau_{FrR/OcR}(f, t) = 1$ , the signals  $FrR(t)$  and  $OcR(t)$  are fully synchronous at time  $t$  and frequency  $f$ . In the case of maximum synchronization for a certain band  $\Delta f_k$ , the activity in two ECoG channels practically coincided with each other in this frequency band. Conversely, in the case of zero bicoherence,  $\tau_{FrR/OcR}(f, t) = 0$ , the signals exhibit a completely asynchronous mode, then neural ensembles demonstrate significantly different oscillatory dynamics within this frequency band. The value  $\tau_{FrR/OcR}(f, t)$ , changing within the given boundary values  $[0; 1]$ , provides complete information about the connectivity of signals on the time-frequency plane  $(f; t)$ .

We considered the integral bicoherence calculated from pairs of ECoG signals in seven frequency ranges,  $\Delta f_k = [f_1^k; f_2^k]$ , Hz, as:

$$\tau^{\Delta f_k}(t) = \frac{1}{\Delta f_k} \int_{f_1^k}^{f_2^k} \tau(f, t) \cdot df, \tag{8}$$

where  $k = 1 \dots 7$  number of the considered frequency range (see Table 1).

In this case, seven dependences  $\tau^{\Delta f_k}(t)$  were calculated for each pair of ECoG signals. Figure 2

**Table 1** Characteristics of frequency ranges for assessing the integral bicoherence of ECoG signals

frequency band	Band minimum, $f_1^k$ , Hz	Band maximum, $f_2^k$ , Hz	Band length, $\Delta f_k$ , Hz
$\Delta f_1$	0.5	1.5	1
$\Delta f_2$	1	4	3
$\Delta f_3$	5	9	4
$\Delta f_4$	9	12	3
$\Delta f_5$	10	14	4
$\Delta f_6$	12	14	2
$\Delta f_7$	14	20	6

(Step2) shows five similar dependencies for signal fragments,  $FrR(t)$  and  $OcR(t)$ . In conclusion, for each such dependence, we carried out a statistical analysis of the given quantity  $\tau^{\Delta f_k}(t)$ , i. e., estimated the mean, median, 25–75 % of the distribution, maximum/minimum spread, as shown in Fig. 2, Step 3.

### 2.4 Statistical analysis

Distribution of bilateral and unilateral synchronization values were tested for normality (per each age, each band, each state) with Kolmogorov–Smirnov test that displayed  $p > 0.05$ , suggesting a normal distribution. Statistical analysis was performed using ANOVA, repeated measures ANOVA and Bonferroni post hoc test.

## 3 Results

### 3.1 Age-related dynamics of absence epilepsy (determining of epileptic phenotypes)

Visual analysis of ECoG in the group of WAG/Rij rats displayed a strong between-subject variability of spike-wave activity. The presence/absence of genuine SWDs in ECoG during the analyzed 3 h period was used as a criterion to split the group in two phenotypes (epileptic and non-epileptic correspondingly). Animals of different phenotypes showed no other physical and/or behavioral differences. Six out of ten rats showed only a few abortive SWDs at the age of 5 and 9 months ( $n = 6$  rats, non-epileptic phenotype, Fig. 3A). The rest 4 rats that showed very few SWDs at the age of 5 months (from 0 to 5 SWDs per 3 h, Fig. 3A) and a substantial number of SWDs at the age of 9 months (from 22 to 41 per 3 h) were classified as rats with the epileptic phenotype. The factor of “Age” significantly affected the number of SWDs (RM ANOVA,  $F_{1,8} = 58.5, p < 0.0001$ ) with significant “Age”\*“Phenotype” interactions ( $F_{1,8} = 55.8, p < 0.0001$ ). The total duration of SWDs demonstrated the same age-related dynamics (RM ANOVA for “Age”

factor  $F_{1,8} = 46.2, p < 0.0005$ ; “Age”\*“Phenotype”  $F_{1,8} = 45.6, p < 0.0005$ ). Bonferroni post hoc test indicated that 9 months old epileptic rats had significantly higher number of SWDs and higher total SWDs duration than at the age of 5 months; and that non-epileptic rats demonstrated at both ages (both  $p$ ’s  $< 0.05$ , Table 2).

At the age of 5 months, epileptic rats and non-epileptic rats did not show significant differences in the number and the total duration of SWDs (Table 2). Therefore, it is assumed that 5 months old epileptic rats were on the preclinical stage of absence epilepsy and showed very few abortive SWDs (from 0 to 5 SWDs per 3 h, Fig. 3 A) which were similar to abortive SWDs in non-epileptic rats (Table 2). Nine months old epileptic rats demonstrated fully blown SWDs, i. e. the clinical stage of absence epilepsy.

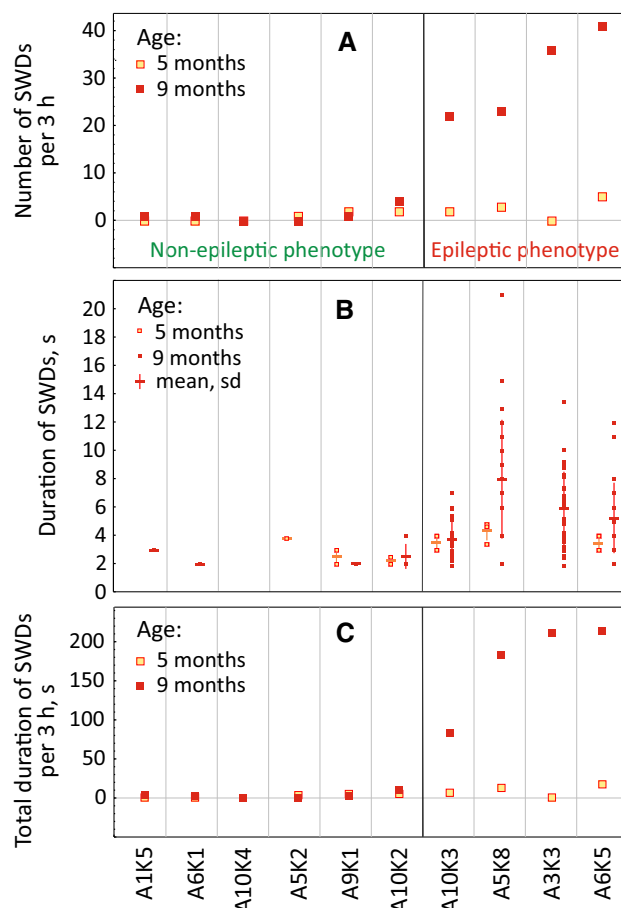


**Fig. 3** Quantitative parameters of SWDs in the group of WAG/Rij rats: age-related dynamics of individual data of 6 non-epileptic and 4 epileptic rats: **A** number of SWDs; **B** duration of single SWDs; **C** total duration of SWDs. SWDs were detected automatically during a 3 h interval at the beginning of the dark period (21:00–23:59)

**Table 2** Descriptive data of epileptic spike-wave discharges in ECoG as measured during 3-h period (mean and standard deviation)

	Non-epileptic phenotype		Epileptic phenotype	
	Age = 5 m	Age = 9 m	Age = 5 m	Age = 9 m
Number of SWDs	0.83 ± 0.98	1.17 ± 1.47	2.05 ± 2.08	30.50 ± 9.49*
Total duration, s	2.22 ± 2.46	2.83 ± 3.71	9.20 ± 7.38	172.67 ± 61.52*
Mean duration of SWDs, s	2.38 ± 0.18	2.38 ± 0.18	2.25 ± 0.35	5.65 ± 2.13*

\*Significantly higher than values measured in epileptic phenotype at the age of 5 months old; and than values measured in non-epileptic rats at both ages (Bonferroni post hoc test,  $p < 0.05$ )

### 3.2 Intracortical synchronization pattern

To characterize bilateral intracortical synchronization, wavelet bicoherence was computed between two symmetrical frontal left and right ECoG channels. Analysis was performed separately for the state of Wake/REM sleep and NREM sleep (states were automatically detected, see Sect. 2.1). Fig. 4 shows the differences in wavelet bicoherence between the two phenotypes.

During the state of Wake/REM sleep, 110 epochs were analyzed in non-epileptic rats (55 epochs at the age of 5 months and 55 epochs—9 months) and 69 epochs in epileptic rats (20 epochs in of 5-m old rats and 49 epochs—in 9-m old rats, Fig. 4A). During the state of NREM sleep, 105 epochs were analyzed in non-epileptic rats (52 epochs at the age of 5 months and 53 epochs—9 months) and 72 epochs in epileptic rats (23 epochs at the age of 5-m and 49 epochs—9-m, Fig. 4B).

#### 3.2.1 Bilateral synchronization

During Wake/REM sleep, the factor of “Phenotype” was not significant at the age of 5 months, indicating that bilateral synchronization in epileptic and non-epileptic rats did not differ (Fig. 4A). At the age of 9 months, significant effect of “Phenotype” (ANOVA,  $F_{1;714} = 75.0$ ,  $p < 0.0001$ ) indicated that bilateral synchronization in epileptic rats was lower than in non-epileptics in particular frequency bands (0.5–1.5 Hz, 5–9 Hz and 10–20 Hz,  $p < 0.05$ , Bonferroni post hoc test).

During NREM sleep, the factor of “Phenotype” significantly affected synchronization values at the age of 5 months (ANOVA,  $F_{1;511} = 11.5$ ,  $p < 0.001$ , Fig. 4B): bilateral synchronization in epileptic rats was lower than in non-epileptics. The effect of “Band” was also significant (ANOVA,  $F_{6;511} = 5.5$ ,  $p < 0.001$ ); therefore, differences in some bands were sharper than in others. At the age of 9 months, the significance of “Phenotype” factor was very high ( $F_{1;700} = 33.6$ ,  $p < 0.00001$ ), as well as the significance of ‘Band’ factor ( $F_{6;700} = 31.1$ ,  $p < 0.00001$ ) with significantly lower values in 10–14; 12–14 and 14–20 Hz in epileptic rats (all  $p$ 's < 0.05, Bonferroni post hoc test, Fig. 4A).

#### 3.2.2 Unilateral synchronization

Statistical results of unilateral synchronization values are shown in Table 4, where the number of episodes and categories are the same as that shown in Table 3.

During Wake/REM sleep (Fig. 5A), the factor “Phenotype” did not affect unilateral synchronization.

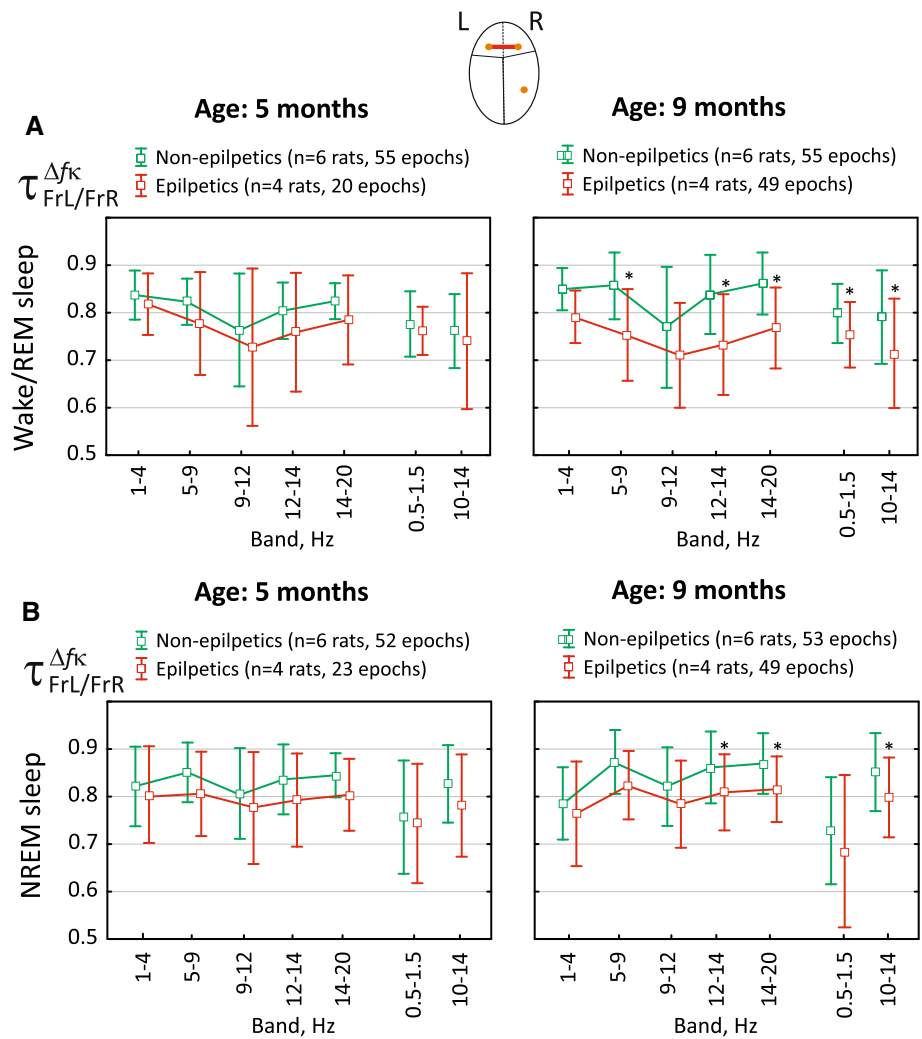
During NREM sleep as early as at the age of 5 months, the factor “Phenotype” was significant (ANOVA,  $F_{1;511} = 25.1$ ,  $p < 0.0001$ ), suggesting that synchronization in epileptic rats was lower than in non-epileptics. The effect of ‘Band’ was also significant (ANOVA,  $F_{6;511} = 8.9$ ,  $p < 0.0001$ ), suggesting that differences in some bands were sharper than in others. At the age of 9 months, ‘Phenotype’ factor was not significant ( $F_{1;714} = 0.3$ ,  $p = 0.59$ , Fig. 5 A).

## 4 Discussion

The present paper describes results of intracortical synchronization in low frequency bands in epileptic and non-epileptic WAG/Rij rats. Intracortical synchronization pattern was assessed by measuring values of wavelet bicoherence during interictal periods in non-overlapping frequency bands (1–4–5–9–12–14–20 Hz). Based in our current results, defined age-related and state-related differences of synchronization pattern in two groups of rats with different epileptic profile.

Here we draw attention to three key points: wavelet bicoherence for analysis of ECoG data; intracortical synchronization pattern; preclinical state of age-dependent progression of absence epilepsy. First, wavelet bicoherence is now the method of choice for qualitatively evaluating the coherence and timing of complex non-stationary signals. Despite some complications of numerical calculations compared to classical linear measures for estimating the Fourier frequency and signal phase, wavelet bicoherence is a more reliable method for processing short nonstationary time series of biomedical data. In addition, this method demonstrates high performance in noisy and unstable signals. Besides this, wavelet bicoherence is computed in predetermined frequency bands, therefore, results of wavelet bicoherence analysis could be interpreted as frequency-dependent synchronization pattern.

**Fig. 4** Bilateral intracortical synchronization (i. e., values of wavelet bicoherence) as measured during Wake/REM sleep (A) and NREM sleep (B) in epileptic and non-epileptic WAG/Rij rats (mean and SD). Lines interconnecting synchronization values in non-overlapping frequency bands. \*Significant differences (Bonferroni post hoc test,  $p < 0.05$ )



We define intracortical synchronization pattern as a consolidated estimate of wavelet bicoherence in frequencies 0.5–20 Hz. Figure 6 demonstrates that frequency profiles of bi- and unilateral synchronization patterns are state-dependent, epilepsy-dependent and age dependent. Fronto-frontal synchronization pattern (Fig. 6A) has merely changed with age, and non-epileptic rats showed higher value of coherence than epileptic rats in Wake/REM sleep and NREM sleep. Fronto-occipital synchronization pattern (Fig. 6B) has changed with age in non-epileptic rats, especially during Wake/REM sleep (age-related decrease in coherence values). Similar plots of synchronization pattern might be used as diagnostic maps and used for early diagnosis of absence epilepsy in predisposed subjects.

Third, particular attention was given to age-dependent progression of absence epilepsy and to the preclinical state in 5-m old epileptic rats, when only few immature SWDs were detected; in contrast to the clinical stage at age of 9-months in the same subjects, when the averaged number of SWDs was ~ 30 per 3 h. It is important to note that a lower unilateral fronto-occipital wavelet bicoherence was defined only

on the preclinical stage of epileptic rats (5-months old), but differences were no longer present at the clinical stage (9-months old). Therefore, a reduction of fronto-occipital synchronization may be a sign of early epileptogenesis in genetically predisposed subjects. Another remarkable point is that fronto-occipital synchronization at the preclinical state reduced in narrow frequency bands: 5–9 Hz and 10–14 Hz. 5–9 Hz oscillations are typical for ECoG in rats, and these oscillations are triggered by the cortical part of the thalamo-cortical network [52]; and in pathological conditions they could be transformed to epileptic SWDs [12]. Alpha frequencies (10–14 Hz) are known to be produced by the thalamic part of thalamo-cortical circuitry [53, 54]. Therefore reduced fronto-occipital synchronization in 5–9 Hz and in 10–14 Hz during NREM sleep on the preclinical state of absence epilepsy may be (1) interpreted as a marker of thalamo-cortical impairment and (2) may be associated with epileptogenic processes underlying long-term progression of absence epilepsy. A low value of unilateral synchronization in 5–9 Hz, 9–12 Hz and 10–14 Hz during NREM sleep might be interpreted as a sign of bad prognosis in genetically prone subjects.

**Table 3** Values of bilateral intracortical synchronization (mean and standard deviation)

State	Band, Hz	Age = 5 m		Age = 9 m	
		Non-epileptic	Epileptic	Non-epileptic	Epileptic
Wake/REM sleep	0.5–1.5	0.77 ± 0.07	0.76 ± 0.05	0.80 ± 0.06	0.76 ± 0.07
	1–4	0.81 ± 0.05	0.82 ± 0.06	0.82 ± 0.04	0.79 ± 0.06
	5–9	0.80 ± 0.05	0.78 ± 0.11	0.83 ± 0.07	0.75 ± 0.10*
	9–12	0.74 ± 0.12	0.73 ± 0.17	0.74 ± 0.13	0.71 ± 0.11
	10–14	0.76 ± 0.08	0.74 ± 0.14	0.79 ± 0.10	0.72 ± 0.12*
	12–14	0.78 ± 0.06	0.76 ± 0.12	0.81 ± 0.08	0.73 ± 0.11*
	14–20	0.80 ± 0.04	0.78 ± 0.09	0.83 ± 0.07	0.77 ± 0.09*
	Total	0.78 ± 0.07	0.77 ± 0.11	0.80 ± 0.09	0.75 ± 0.10 <sup>#</sup>
NREM sleep	0.5–1.5	0.75 ± 0.12	0.75 ± 0.13	0.72 ± 0.11	0.69 ± 0.16
	1–4	0.82 ± 0.08	0.80 ± 0.10	0.78 ± 0.08	0.76 ± 0.11
	5–9	0.85 ± 0.06	0.81 ± 0.09	0.87 ± 0.07	0.82 ± 0.07
	9–12	0.80 ± 0.10	0.78 ± 0.12	0.82 ± 0.08	0.78 ± 0.09
	10–14	0.82 ± 0.08	0.78 ± 0.11	0.85 ± 0.08	0.80 ± 0.08*
	12–14	0.83 ± 0.07	0.79 ± 0.10	0.86 ± 0.08	0.81 ± 0.08*
	14–20	0.84 ± 0.05	0.80 ± 0.08	0.87 ± 0.06	0.82 ± 0.07*
	Total	0.82 ± 0.09	0.79 ± 0.10 <sup>#</sup>	0.82 ± 0.09	0.78 ± 0.11 <sup>#</sup>

\*Significant differences between epileptic and non-epileptics (Bonferroni post-hoc test,  $p < 0.05$ )

<sup>#</sup>Significant effect of “Phenotype” factor (ANOVA,  $p < 0.05$ )

**Table 4** Values of unilateral synchronization (mean and standard deviation)

State	Band, Hz	Age = 5 m		Age = 9 m	
		Non-epileptic	Epileptic	Non-epileptic	Epileptic
Wake/REM sleep	0.5–1.5	0.44 ± 0.13	0.41 ± 0.07	0.40 ± 0.12	0.40 ± 0.12
	1–4	0.45 ± 0.06	0.39 ± 0.08	0.39 ± 0.10	0.42 ± 0.09
	5–9	0.51 ± 0.03	0.48 ± 0.03	0.48 ± 0.07	0.48 ± 0.05
	9–12	0.50 ± 0.12	0.47 ± 0.14	0.42 ± 0.07	0.41 ± 0.11
	10–14	0.50 ± 0.06	0.46 ± 0.07	0.46 ± 0.07	0.44 ± 0.07
	12–14	0.49 ± 0.04	0.45 ± 0.04	0.45 ± 0.07	0.45 ± 0.06
	14–20	0.48 ± 0.02	0.45 ± 0.04	0.46 ± 0.07	0.45 ± 0.04
	Total	0.48 ± 0.08	0.45 ± 0.08	0.44 ± 0.09	0.43 ± 0.09
NREM sleep	0.5–1.5	0.43 ± 0.14	0.40 ± 0.09	0.38 ± 0.10	0.38 ± 0.12
	1–4	0.43 ± 0.07	0.40 ± 0.07	0.39 ± 0.11	0.38 ± 0.08
	5–9	0.52 ± 0.04	0.46 ± 0.02*	0.49 ± 0.06	0.49 ± 0.03
	9–12	0.45 ± 0.05	0.41 ± 0.05	0.42 ± 0.08	0.43 ± 0.06
	10–14	0.50 ± 0.05	0.43 ± 0.03*	0.46 ± 0.06	0.47 ± 0.04
	12–14	0.50 ± 0.04	0.43 ± 0.02*	0.46 ± 0.06	0.46 ± 0.04
	14–20	0.50 ± 0.03	0.44 ± 0.03	0.47 ± 0.07	0.47 ± 0.03
	Total	0.48 ± 0.08	0.42 ± 0.06 <sup>#</sup>	0.44 ± 0.09	0.44 ± 0.08

\*Significant differences between epileptic and non-epileptics (Bonferroni post-hoc test,  $p < 0.05$ )

<sup>#</sup>Significant effect of “Phenotype” factor (ANOVA,  $p < 0.05$ )



**Fig. 5** Unilateral intracortical synchronization (i. e., values of wavelet bicoherence) as measured during Wake/REM sleep (A) and NREM sleep (B) in epileptic and non-epileptic WAG/Rij rats (mean and SD). Lines interconnecting synchronization values in non-overlapping frequency bands. \*Significant differences (Bonferroni post hoc test,  $p < 0.05$ )

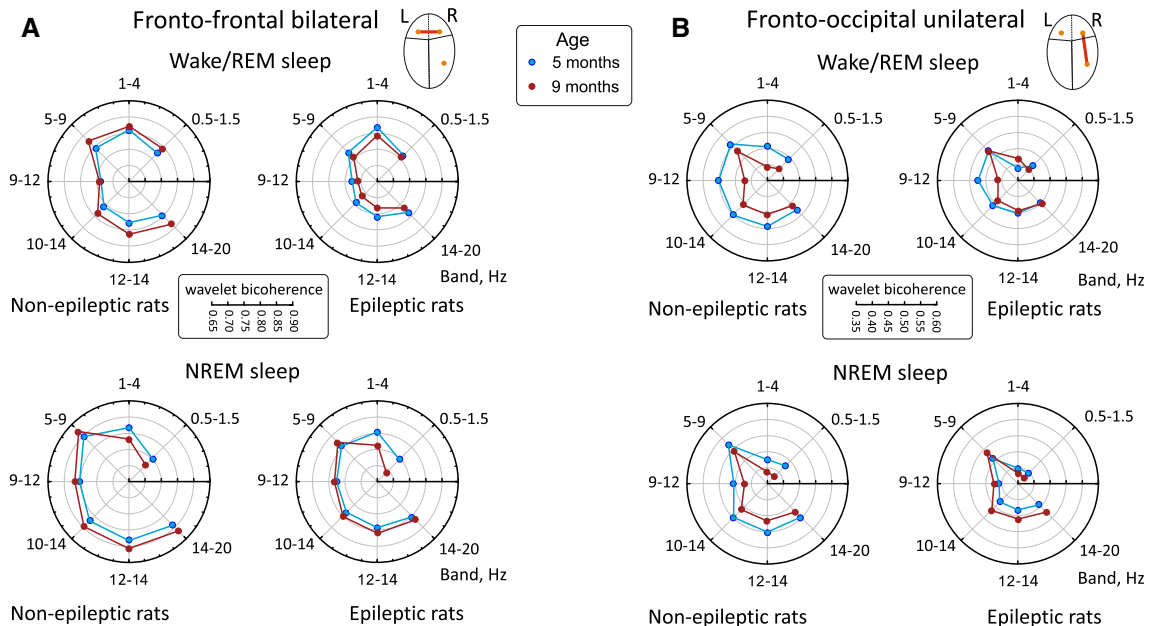
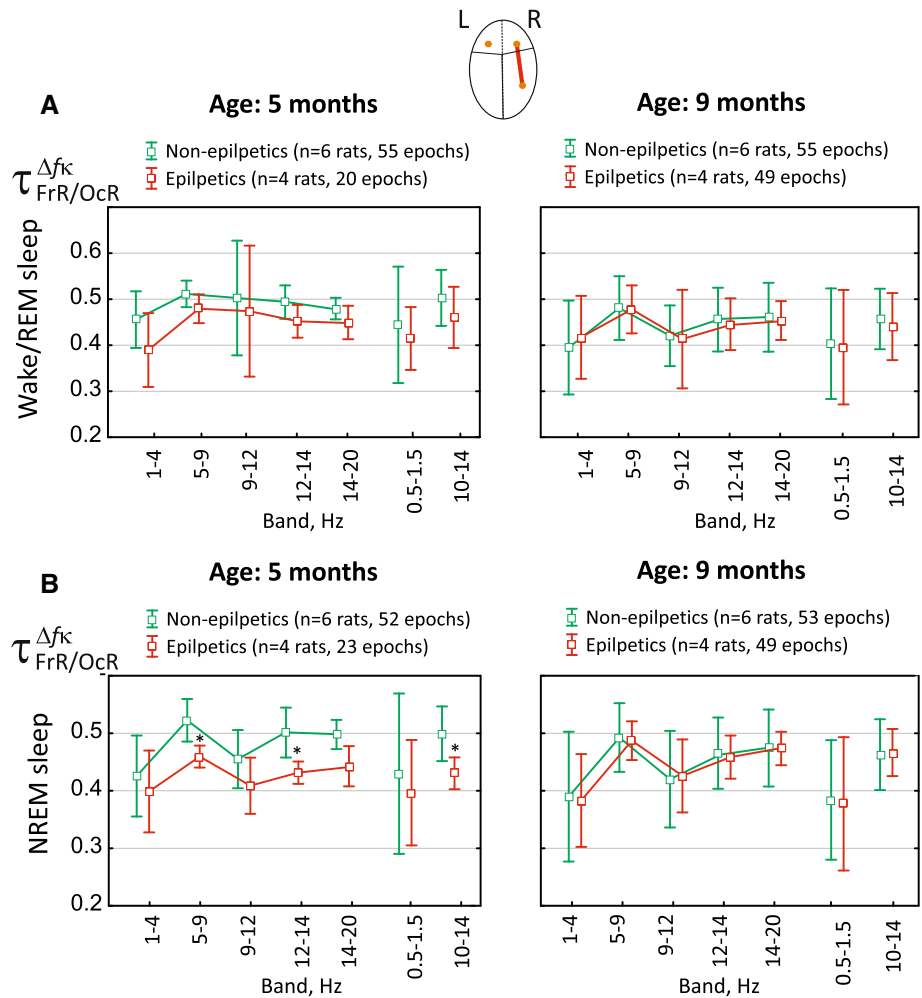


**Fig. 6** Age-related changes of intracortical synchronization in WAG/Rij rats with two different phenotypes. **A** Wavelet bicoherence measured between channels  $FrL(t)$  and  $FrR(t)$  in frequency bands 0.5–20 Hz. **B** Wavelet bicoherence in frequency bands 0.5–20 Hz between channels  $FrR(t)$  and  $OcR(t)$

In other words, an early sign of further development of epileptic activity that might require attention in childhood epilepsy.

It was not surprising that bilateral synchronization during Wake/REM sleep was significantly lower in the epileptic phenotype only at clinical stage and did not differ from values obtained in non-epileptic subjects at the preclinical stage. This fits well to results obtained in patients with childhood absence epilepsy (CAE), which showed a decrease in resting-state functional connectivity bilaterally in the medial pre-frontal cortex, angular gyrus, and inferior parietal lobule in comparison to healthy control; yet an increased connectivity has not been defined in CAE patients [55]. Also the whole brain resting-state functional connectivity in CAE patients indicated a reduced connectivity between the thalamus and cortex [56]. Similarly, Kim et al. in 2014 in patients with idiopathic generalized epilepsy demonstrated a greater reduction of medial prefrontal functional connectivity in relation to increasing disease duration [8]. Their data suggested that thalamoprefrontal network abnormality in these patients is a consequence of the long-standing burden of the disease. Majority of human studies indicated a decrease of thalamo-cortical and bilateral intracortical connectivity, and this decrease may provide a functional basis for cognitive dysfunction in absence epilepsy [17, 55, 56]. It is worth mentioning opposite results. First, EEG-fMRI studies of resting functional connectivity in patients with CAE demonstrated an increase of bilateral connectivity in the lateral orbitofrontal cortex in comparison to normal controls [57]. Second, fMRI-based analysis in WAG/Rij rats demonstrated that regions in which seizures are most intense show markedly increased resting functional connectivity in epileptic WAG/Rij rats compared to Wistar control rats [58]. Inconsistency may be explained by specificity of fMRI-based methodology, different sub-syndromes of generalized genetic/idiopathic epilepsy, “influences of age and medications, and physiological changes, as well as errors introduced by certain pre-processing steps” [17]. Indeed, Xu et al. in 2013 demonstrated a significant divergence of functional connectivity within and between brain modules in patients with absence epilepsy: nodes in the limbic system, including the amygdala and the putamen, showed a decreased functional connections to the default mode network; in contrast, the connections to somatosensory system were increased [18].

## 5 Conclusion

WAG/Rij rats were genetically predisposed to absence epilepsy, but there was a biodiversity among these subjects. Here we used spike-wave seizures in ECoG as the hallmark of absence epilepsy, and defined epileptic and non-epileptic phenotype. Epileptic subjects showed fully blown spike-wave seizures at the age of 9 months

(clinical stage) and only a few immature seizures (pre-clinical stage). Bilateral synchronization (fronto-frontal pair) and unilateral synchronization (fronto-occipital pair) was computed using wavelet bicoherence. We made the following conclusions.

1. Only on the clinical stage of absence epilepsy, bilateral fronto-frontal synchronization in epileptic subjects was lower than in non-epileptic ones. A reduced synchronization was defined during both “healthy” periods: Wake/REM sleep and NREM sleep.
2. Only on preclinical stage of absence epilepsy, unilateral fronto-occipital synchronization in epileptic rats was lower than in non-epileptic ones. A reduced synchronization was defined only during NREM sleep and in specific frequency bands—alpha (10–14 Hz) and 5–9 Hz.
3. A reduction of fronto-occipital synchronization may be a sign of early epileptogenesis in genetically predisposed subjects. Five-9 Hz oscillations are typical for ECoG in rats, and these oscillations are triggered by the cortical part of the thalamo-cortical network [52]; and in pathological conditions they could be transformed to epileptic SWDs [12]. Alpha frequencies (10–14 Hz) are known to be produced by the thalamic part of thalamo-cortical circuitry [53, 54]. Reduced fronto-occipital synchronization in 5–9 Hz and in 10–14 Hz in epileptic WAG/Rij rats on the preclinical state of absence epilepsy may be (1) interpreted as a marker of thalamo-cortical impairment and (2) may be associated with epileptogenic processes underlying long-term progression of absence epilepsy.

**Acknowledgements** This work has been supported by the RF Government Grant No. 075-15-2022-1094 in part of the biophysical interpretation. In the part of the development of numeric method of data analysis, this work has been supported by of the Government Procurement of the Russian Federation Ministry of Healthcare No. 056-00030-21-01 of May 02, 2021 Theoretical and Experimental Study of the Integrative Activity of Various Physiological Systems of Patient under Stress (the State registration number 121030900357-3). The experimental work was carried out with the support of the Ministry of Education and Science of the Russian Federation within the state assignment of Institute of Higher Nervous Activity for 2021–2023.

**Data Availability Statement** The datasets generated during and analysed during the current study are available from the corresponding author on reasonable request.

## References

1. I.E. Scheffer, S. Berkovic, G. Capovilla, M.B. Connolly, J. French, L. Guilhoto, E. Hirsch, S. Jain, G.W. Mathern, S.L. Moshé et al., ILAE classification of the epilepsies: position paper of the ILAE commission for classification and terminology. *Epilepsia* **58**(4), 512–521 (2017)
2. R.S. Fisher, J.H. Cross, J.A. French, N. Higurashi, E. Hirsch, F.E. Jansen, L. Lagae, S.L. Moshé, J. Peltola, E. Roulet Perez et al., Operational classification of seizure types by the international league against epilepsy: Position paper of the ILAE commission for classification and terminology. *Epilepsia* **58**(4), 522–530 (2017)
3. S. Matricardi, A. Verrotti, F. Chiarelli, C. Cerminara, P. Curatolo, Current advances in childhood absence epilepsy. *Pediatr. Neurol.* **50**(3), 205–212 (2014)
4. S.A. Mullen, S.F. Berkovic, I.G. Commission, S.F. Berkovic, D.H. Lowenstein, M. Kato, H. Cross, P. Satishchandra, P. De Jonghe, A. Goldman et al., Genetic generalized epilepsies. *Epilepsia* **59**(6), 1148–1153 (2018)
5. C.P. Panayiotopoulos, Typical absence seizures and related epileptic syndromes: assessment of current state and directions for future research. *Epilepsia* **49**(12), 2131–2139 (2008)
6. H. Blumenfeld, Cellular and network mechanisms of spike-wave seizures. *Epilepsia* **46**, 21–33 (2005)
7. V. Crunelli, M.L. Lőrincz, C. McCafferty, R.C. Lambert, N. Leresche, G. Di Giovanni, F. David, Clinical and experimental insight into pathophysiology, comorbidity and therapy of absence seizures. *Brain* **143**(8), 2341–2368 (2020)
8. J.B. Kim, S.-I. Suh, W.-K. Seo, K. Oh, S.-B. Koh, J.H. Kim, Altered thalamocortical functional connectivity in idiopathic generalized epilepsy. *Epilepsia* **55**(4), 592–600 (2014)
9. G. Kozák, T. Földi, A. Berényi, Spike-and-wave discharges are not pathological sleep spindles, network-level aspects of age-dependent absence seizure development in rats. *Eneuro* (2020). <https://doi.org/10.1523/ENEURO.0253-19.2019>
10. N. Leresche, R.C. Lambert, A.C. Errington, V. Crunelli, From sleep spindles of natural sleep to spike and wave discharges of typical absence seizures: is the hypothesis still valid? *Pflügers Arch. Eur. J. Physiol.* **463**(1), 201–212 (2012)
11. A. Lüttjohann, G. van Luijtelaar, Dynamics of networks during absence seizure's on-and offset in rodents and man. *Front. Physiol.* **6**, 16 (2015)
12. D. Pinault, M. Vergnes, C. Marescaux, Medium-voltage 5–9-hz oscillations give rise to spike-and-wave discharges in a genetic model of absence epilepsy: in vivo dual extracellular recording of thalamic relay and reticular neurons. *Neuroscience* **105**(1), 181–201 (2001)
13. E. Sitnikova, Thalamo-cortical mechanisms of sleep spindles and spike-wave discharges in rat model of absence epilepsy (a review). *Epilepsy Res.* **89**(1), 17–26 (2010)
14. G. van Luijtelaar, On the yin and yang of spike and waves. *J. Physiol.* **598**(12), 2279–2280 (2020)
15. E. Sitnikova, G. van Luijtelaar, Cortical and thalamic coherence during spike-wave seizures in wag/rij rats. *Epilepsy Res.* **71**(2–3), 159–180 (2006)
16. M. Sysoeva, A. Lüttjohann, G. van Luijtelaar, I. Sysoev, Dynamics of directional coupling underlying spike-wave discharges. *Neuroscience* **314**, 75–89 (2016)
17. P.W. Carney, G.D. Jackson, Insights into the mechanisms of absence seizure generation provided by EEG with functional MRI. *Front. Neurol.* **5**, 162 (2014)
18. C.-P. Xu, S.-W. Zhang, T. Fang, M. Manxiu, Q. Chen-can, C. Huaifu, H.-W. Zhu, Y.-J. Li, L. Zuxiang, Altered functional connectivity within and between brain modules in absence epilepsy: a resting-state functional magnetic resonance imaging study. *BioMed Res. Int.* **2013**, 734893 (2013)
19. M. Sifuzzaman, M.R. Islam, M. Ali, *Application of wavelet transform and its advantages compared to Fourier transform* (Vidyasagar University, Midnapore, 2009)
20. K. Kato, K. Takahashi, N. Mizuguchi, J. Ushiba, Online detection of amplitude modulation of motor-related EEG desynchronization using a lock-in amplifier: Comparison with a fast Fourier transform, a continuous wavelet transform, and an autoregressive algorithm. *J. Neurosci. Methods* **293**, 289–298 (2018)
21. P.S. Addison, *Introduction to redundancy rules: the continuous wavelet transform comes of age* (The Royal Society Publishing, London, 2018)
22. W. Zeng, M. Li, C. Yuan, Q. Wang, F. Liu, Y. Wang, Identification of epileptic seizures in EEG signals using time-scale decomposition (ITD), discrete wavelet transform (DWT), phase space reconstruction (PSR) and neural networks. *Artif. Intell. Rev.* **53**(4), 3059–3088 (2020)
23. D. Bhati, R.B. Pachori, M. Sharma, V.M. Gadre, Automated detection of seizure and nonseizure EEG signals using two band biorthogonal wavelet filter banks, in *Biomedical signal processing*. (Springer, Berlin, 2020), pp.137–155
24. K. Sergeev, A. Runnova, M. Zhuravlev, O. Kolokolov, N. Akimova, A. Kiselev, A. Titova, A. Slepnev, N. Semenova, T. Penzel, Wavelet skeletons in sleep EEG-monitoring as biomarkers of early diagnostics of mild cognitive impairment. *Chaos* **31**(7), 073110 (2021)
25. A. Runnova, M. Zhuravlev, R. Ukolov, I. Blokhina, A. Dubrovski, N. Lezhnev, E. Sitnikova, E. Saranceva, A. Kiselev, A. Karavaev et al., Modified wavelet analysis of ECOG-pattern as promising tool for detection of the blood-brain barrier leakage. *Sci. Rep.* **11**(1), 1–8 (2021)
26. A. Coenen, E. Van Luijtelaar, Genetic animal models for absence epilepsy: a review of the wag/rij strain of rats. *Behav. Genet.* **33**(6), 635–655 (2003)
27. E. Van Luijtelaar, A. Coenen, Two types of electrocortical paroxysms in an inbred strain of rats. *Neurosci. Lett.* **70**(3), 393–397 (1986)
28. G. van Luijtelaar, F.Y. Onat, M.J. Gallagher, Animal models of absence epilepsies: what do they model and do sex and sex hormones matter? *Neurobiol. Dis.* **72**, 167–179 (2014)
29. G. Van Luijtelaar, G. Van Oijen, Establishing drug effects on electrocorticographic activity in a genetic absence epilepsy model: advances and pitfalls. *Front. Pharmacol.* **11**, 395 (2020)
30. E. Sitnikova, A.E. Hramov, V. Grubov, A.A. Koronovsky, Rhythmic activity in EEG and sleep

- in rats with absence epilepsy. *Brain Res. Bull.* **120**, 106–116 (2016)
31. E. Sitnikova, Neonatal sensory deprivation promotes development of absence seizures in adult rats with genetic predisposition to epilepsy. *Brain Res.* **1377**, 109–118 (2011)
  32. E. Sitnikova, A.E. Hramov, V. Grubov, A.A. Koronovsky, Age-dependent increase of absence seizures and intrinsic frequency dynamics of sleep spindles in rats. *Neurosci J* **2014** (2014)
  33. E. Sitnikova, E.M. Rutsikova, V.V. Raevsky, Reduction of epileptic spike-wave activity in wag/rij rats fostered by wistar dams. *Brain Res.* **1594**, 305–309 (2015)
  34. E.Y. Sitnikova, K. Smirnov, V. Grubov, A. Hramov, Diagnostic principles of immature epileptic (proepileptic) eeg activity in rats with genetic predisposition to absence epilepsy. *Inform. Control Syst.* **1**, 89–97 (2019)
  35. P. Halász, A. Kelemen, A. Szűcs, The role of nrem sleep micro-arousals in absence epilepsy and in nocturnal frontal lobe epilepsy. *Epilepsy Res.* **107**(1–2), 9–19 (2013)
  36. P. Halász, M. Terzano, L. Parrino, Spike-wave discharge and the microstructure of sleep-wake continuum in idiopathic generalised epilepsy. *Neurophysiologie Clinique* **32**(1), 38–53 (2002)
  37. E. Sitnikova, A.E. Hramov, V.V. Grubov, A.A. Ovchinnikov, A.A. Koronovsky, On-off intermittency of thalamo-cortical oscillations in the electroencephalogram of rats with genetic predisposition to absence epilepsy. *Brain Res.* **1436**, 147–156 (2012)
  38. M.K. Smyk, I.V. Sysoev, M.V. Sysoeva, G. van Luijckelaar, W.H. Drinkenburg, Can absence seizures be predicted by vigilance states? Advanced analysis of sleep-wake states and spike-wave discharges' occurrence in rats. *Epilepsy Beh.* **96**, 200–209 (2019)
  39. M.K. Smyk, G. Van Luijckelaar, Circadian rhythms and epilepsy: a suitable case for absence epilepsy. *Front. Neurol.* **11**, 245 (2020)
  40. G. van Luijckelaar, A. Bikbaev, Midfrequency cortico-thalamic oscillations and the sleep cycle: genetic, time of day and age effects. *Epilepsy Res.* **73**(3), 259–265 (2007)
  41. M. Zhuravlev, A. Runnova, K. Smirnov, E. Sitnikova, Spike-wave seizures, nrem sleep and micro-arousals in wag/rij rats with genetic predisposition to absence epilepsy: Developmental aspects. *Life* **12**(4), 576 (2022)
  42. A. Runnova, M. Zhuravlev, A. Kiselev, R. Ukolov, K. Smirnov, A. Karavaev, E. Sitnikova, Automatic wavelet-based assessment of behavioral sleep using multichannel electrocorticography in rats. *Sleep Breath.* **25**(4), 2251–2258 (2021)
  43. K. Schiecke, M. Wacker, F. Benninger, M. Feucht, L. Leistritz, H. Witte, Matching pursuit-based time-variant bispectral analysis and its application to biomedical signals. *IEEE Trans. Biomed. Eng.* **62**(8), 1937–1948 (2015)
  44. L.W. Sheppard, V. Vuksanović, P.V. McClintock, A. Stefanovska, Oscillatory dynamics of vasoconstriction and vasodilation identified by time-localized phase coherence. *Phys. Med. Biol.* **56**(12), 3583 (2011)
  45. M. Le Van Quyen, J. Foucher, J.-P. Lachaux, E. Rodriguez, A. Lutz, J. Martinerie, F.J. Varela, Comparison of Hilbert transform and wavelet methods for the analysis of neuronal synchrony. *J. Neurosci. Methods* **111**(2), 83–98 (2001)
  46. V. Sakkalis, Review of advanced techniques for the estimation of brain connectivity measured with eeg/meg. *Comput. Biol. Med.* **41**(12), 1110–1117 (2011)
  47. V.V. Makarov, M.O. Zhuravlev, A.E. Runnova, P. Protasov, V.A. Maksimenko, N.S. Frolov, A.N. Pisarchik, A.E. Hramov, Betweenness centrality in multiplex brain network during mental task evaluation. *Phys. Rev. E* **98**(6), 062413 (2018)
  48. A.E. Hramov, A.A. Koronovskii, V.A. Makarov, A.N. Pavlov, E. Sitnikova, *Wavelets in neuroscience* (Springer, Berlin, 2015)
  49. A.N. Pavlov, A.E. Hramov, A.A. Koronovskii, Y.E. Sitnikova, V.A. Makarov, A.A. Ovchinnikov, Wavelet analysis in neurodynamics. *Phys. Usp.* **55**(9), 845–875 (2012)
  50. E. Sitnikova, A.E. Hramov, V. Grubov, A.A. Koronovsky, Time-frequency characteristics and dynamics of sleep spindles in wag/rij rats with absence epilepsy. *Brain Res.* **1543**, 290–299 (2014)
  51. A. Bandrivskyy, A. Bernjak, P. McClintock, A. Stefanovska, Wavelet phase coherence analysis: application to skin temperature and blood flow. *Cardiovasc. Eng.* **4**(1), 89–93 (2004)
  52. D. Pinault, Cellular interactions in the rat somatosensory thalamocortical system during normal and epileptic 5–9 hz oscillations. *J. Physiol.* **552**(3), 881–905 (2003)
  53. E. Niedermeyer, Alpha rhythms as physiological and abnormal phenomena. *Int. J. Psychophysiol.* **26**(1), 31–49 (1997). [https://doi.org/10.1016/S0167-8760\(97\)00754-X](https://doi.org/10.1016/S0167-8760(97)00754-X)
  54. S.W. Hughes, V. Crunelli, Thalamic mechanisms of eeg alpha rhythms and their pathological implications. *Neuroscientist* **11**(4), 357–372 (2005)
  55. C. Luo, Q. Li, Y. Lai, Y. Xia, Y. Qin, W. Liao, S. Li, D. Zhou, D. Yao, Q. Gong, Altered functional connectivity in default mode network in absence epilepsy: a resting-state fmri study. *Hum. Brain Mapp.* **32**(3), 438–449 (2011)
  56. R.A. Masterton, P.W. Carney, G.D. Jackson, Cortical and thalamic resting-state functional connectivity is altered in childhood absence epilepsy. *Epilepsy Res.* **99**(3), 327–334 (2012)
  57. X. Bai, J. Guo, B. Killory, M. Vestal, R. Berman, M. Negishi, N. Danielson, E. Novotny, R. Constable, H. Blumenfeld, Resting functional connectivity between the hemispheres in childhood absence epilepsy. *Neurology* **76**(23), 1960–1967 (2011)
  58. A.M. Mishra, X. Bai, J.E. Motelow, M.N. DeSalvo, N. Danielson, B.G. Sanganahalli, F. Hyder, H. Blumenfeld, Increased resting functional connectivity in spike-wave epilepsy in wag/rij rats. *Epilepsia* **54**(7), 1214–1222 (2013)

Springer Nature or its licensor (e.g. a society or other partner) holds exclusive rights to this article under a publishing agreement with the author(s) or other rightsholder(s); author self-archiving of the accepted manuscript version of this article is solely governed by the terms of such publishing agreement and applicable law.